

PARTIAL DISCHARGE (PD) BEHAVIOR OF HIGH VOLTAGE FUSES WITH MODIFIED FILLER

J. Gärtner⁽¹⁾, M. Krins⁽²⁾, E. Gockenbach⁽¹⁾, H. Borsi⁽¹⁾

Institute of Electric Power Systems - Division of High Voltage Engineering (Schering-Institute)⁽¹⁾, University of Hannover, Callinstraße 25A, D-30167 Hannover, Germany, gaertner@rrzn.uni-hannover.de
Siemens AG⁽²⁾, Power Transmission and Distribution, High Voltage, Nonnendammallee 104, D-13629 Berlin, Germany, matthias.krins@siemens.com

Abstract: In conventional current-limiting hv-fuses granular quartz is used as arc quenching filler. The gas filled pore space between the filler’s grains tends to favor PD generation. These PD have been analyzed by means of a phase resolved PD analysis (PRPDA) at different testing conditions (voltage, current, pressure, temperature, gas). A reduction of the PD may be achieved by eliminating the pore space of the filler or by electrical field grading. Pore space was eliminated by filling it with quartz powder, field grading was achieved by enhancing the dielectric properties of the pore’s environment (i.e. the sand). Among the presented modifications clogging with quartz powder is most favorable, since its high impact on PD, low costs and negligible changes to the production process of the fuses. In addition a strong decay of the switching overvoltage was revealed during AC switching tests at critical current I_2 of fuses filled with modified filler.

Keywords: current limiting high voltage fuse, partial discharge behavior, corona, switching overvoltage

1. Introduction

Asset management is a major concern in cost efficient power delivery [1]. Beside others it involves condition-based maintenance, which relates to online monitoring of different quantities, one of them being PD [2]. Since switchgear assemblies – in which fuses are integrated [3, 4] – tend to decrease in size [5], the PD behavior of fuses becomes a growing concern.

PD in the form of *corona* concerns usage of fuses since the early days, because a degeneration of the fusible elements [6] takes place. Modern current-limiting fuses are corona resistant, but a certain quantity of PD still remains, which does not affect the fuses’ characteristics [7]. However it may tamper online monitoring of PD in devices connected to the fuse.

In a previous paper [7] descriptions of some aspects of the PD behavior of hv-fuses are already presented as concepts for PD elimination modifications of the fuse housing and environment are shown. Now, we will focus on a description of the fuses’ PD behavior by means of sophisticated PD

measurement techniques and reduction of PD using filler modifications.

Filler modification is a difficult task, since it directly affects the “heart” of the fuse: the arc-quenching medium. A large number of papers and patents [e.g. 8-19] deal with such modifications, but most of the fuses in use are still filled with ordinary granular quartz. The arc-quenching medium is crucial for the current-limiting behavior of the fuses [e.g. 20-23], because it strongly cools down the arc which appears when the fuse switches. Until switching, the filler also influences the thermal equilibrium of the fuse, which is important for its time-current characteristic (see [24] for an enumeration and discussion of different investigations). After switching, the fuse has to resist the recovery voltage, which consist of a steady-state part [25], maybe 1.5 times higher than the rated phase-to-ground voltage [26] and a transient part being massively affected by the fuse itself. The fuses’ performance depends not only on the filler’s physical and chemical properties, but also on the method used for application [27, 28].

2. Partial discharges: genesis and measurement

It is known from high-voltage engineering, that in cavities inside insulating materials electrical discharges evolve, due to local excess of the electrical breakdown field strength of the medium, which fills the cavities’ volume.

If we suppose the fuse being a cylindrical capacitor, neglecting the helical arrangement of

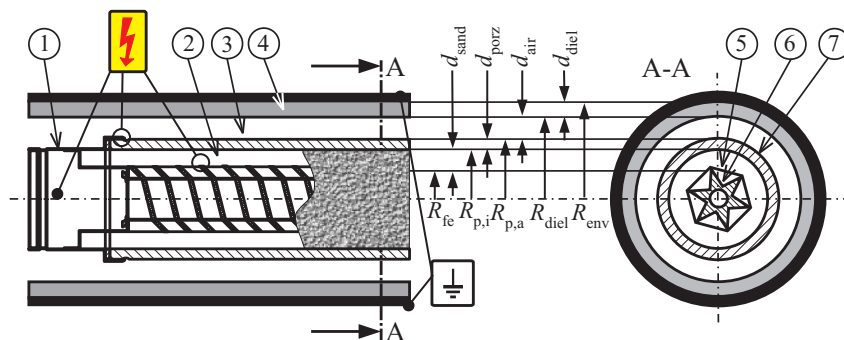


Fig. 1: hv-fuse with encapsulation (schematic): ①: fuse, ②: filler, ③: air gap, ④: dielectric, ⑤: fusible elements, ⑥: fuse’s core, ⑦: porcelain tube.

the fusible elements (⊗ in Fig. 1), the electrical field strength can be calculated by the well known formula for cylindrical capacitors with “stacked dielectrics” [29].

$$\left| \vec{E}_{\text{sand}} \right| = \frac{1}{r \cdot \varepsilon_{\text{sand}}} \cdot \frac{U}{\frac{1}{\varepsilon_{\text{air}}} \cdot \ln\left(\frac{R_{\text{diel}}}{R_{\text{p,a}}}\right) + K} \quad (1)$$

with

$R_{\text{fe}} < r < R_{\text{p,i}}$, radius of interest

$$K = \frac{1}{\varepsilon_{\text{sand}}} \cdot \ln\left(\frac{R_{\text{p,i}}}{R_{\text{fe}}}\right) + \frac{1}{\varepsilon_{\text{porz}}} \cdot \ln\left(\frac{R_{\text{p,a}}}{R_{\text{p,i}}}\right) + \frac{1}{\varepsilon_{\text{diel}}} \cdot \ln\left(\frac{R_{\text{env}}}{R_{\text{diel}}}\right)$$

ε = dielectric constant

R_{fe} = medium radius of fusible elements

$R_{\text{p,i}}, R_{\text{p,a}}$ = inner, outer radius of porcelain tube

R_{diel} = inner radius of dielectric

R_{env} = radius of grounded environment

U = applied voltage .

Obviously, if d_{air} is eliminated ($R_{\text{diel}} = R_{\text{p,a}}$), the el. field becomes maximal for fixed r . This is the reason, why PD may become a future concern, since switchgear assemblies are decreasing in size. Otherwise, this is the simplest technique for PD elimination, since increasing d_{air} decreases the el. field strength. These calculations can only serve as a rough overview, since neglecting the helical arrangement of the fusible elements and their shape leads to underestimation of the real field strength by factor 10-100. An FEM-model reveals a factor of 28, when fusible wire elements with a diameter of 0.15 mm and a length of 600 cm are considered. The calculated field strength at the fusible elements' surface is 13.7 kV/mm for an 6/12 kV, 630 kVA prototype current-limiter, d_{air} being zero, $d_{\text{diel}} = 10$ mm, $R_{\text{p,a}} = 27.5$ mm.

PD measurement and analysis

The well-known PD equivalent circuit [30] shown in Fig. 2 can be explained as follows: The dielectric with void is divided into 3 capacitors: one for the “sane” part (C_1), one for the void (C_2) and one for the dielectric above and under the void (C_3). If an AC voltage is applied, all capacitors will charge, until the void's breakdown voltage is reached. C_2 will discharge resulting in a voltage drop. C_2 will then be

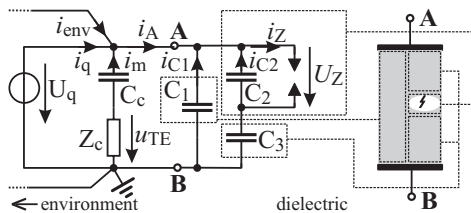


Fig. 2: Equivalent circuit of a PD source.

recharged by the “sane” dielectric C_1 and capacitors outside (e.g. C_c , but also capacitors in the environment i_{env}), until the breakdown voltage is reached again. This may repeat for several times per cycle. PD pulses can be detected through measurement of the charging current of the dielectric himself (serial coupling, i_A) or the current of C_c (parallel coupling, i_m). Since the exact values of the capacitors are unknown (except C_c), the integration of i_m never leads to the exact value of the dispersed charge, but to the so-called *apparent charge* q_a .

Since impulses can be detected outside the dielectric through C_c , they may also be detected by other “capacitors”, such as cables connected to switchgears. Depending on the magnitude of the PD pulses and the damping until they arrive at the cable, sensitive PD measurement may no longer be possible or special techniques [31] must be applied.

If PD impulses are detected in a dielectric, it appeals to know their cause or source. This knowledge can be gained by analysis of different impulse parameters, like their height, length, shape, time of occurrence etc. One of the widely used analysis methods is phase resolved partial discharge analysis (PRPDA) [33, 34], where different PD

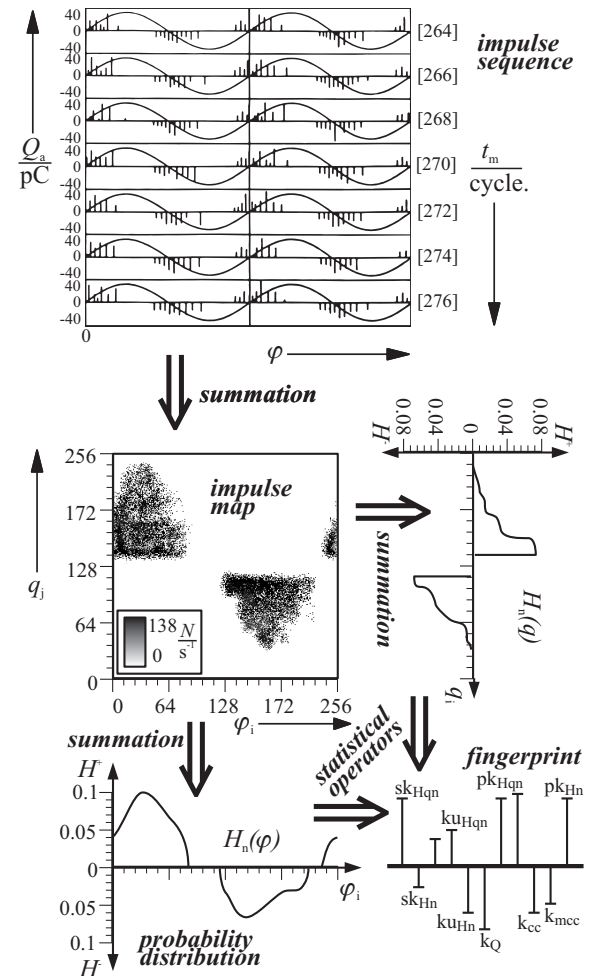


Fig. 3: Scheme of PRPD analysis (meas. data from [32]).

parameters are analyzed with respect to the phase of the supply voltage.

If an AC voltage is supplied to a dielectric with internal faults, PD may occur as shown in Fig. 3. As can be seen, the impulses occur at distinct phases of the AC voltage, with a certain resemblance from cycle to cycle. PRPD-detectors now sum up the amount of impulses in distinct phase windows for a distinct time. This gives a histogram of the amount of impulses vs. phase of test voltage. Eventually, the PRPD-detector is also able to classify the impulses by their apparent charge, so a two-dimensional distribution called *impulse map* \mathbf{M} (Fig. 3) can be formed. In this map each pixel ($m(i,j)$) represents the amount of impulses occurring at phase $\varphi(i)$, with an apparent charge of $q(j)$. Under special conditions, experts are able to distinguish different PD sources by looking to the image of \mathbf{M} , but there are also mathematical and statistical tools available for extraction of features that could be used for classification [35, 36]. PRPD-method gets nowadays completed by impulse sequence analysis [37].

Statistical and mathematical analysis of \mathbf{M}

If the marginal distributions of \mathbf{M} are calculated (Fig. 3), two important distributions are obtained, one being the impulse distribution vs. phase of occurrence $H_n(\varphi)$, the other the impulse distribution vs. apparent charge $H_n(q)$. If the map is multiplied by the calibration vector of the measurement device, the charge map \mathbf{Q} results, which leads to distributions of the charge ($H_q(\varphi)$, $H_q(q)$). Dividing $H_q(\varphi)$ by $H_n(\varphi)$ leads to the mean impulse height $H_{qn}(\varphi)$. If this is still insufficient, \mathbf{Q} can be multiplied by the vector of the test voltage giving \mathbf{E} , the energy map and corresponding distributions. All these distributions may be interpreted as discrete probability functions and treated with statistical tools like formation of momentums (1st momentum being the mean μ , 2nd the divergence σ , 3rd the skewness sk and 4th the kurtosis ku), Weibull analysis etc., or mathematical tools as correlation analysis (giving cross-correlation factors k_c and k_{mcc}), peak detection (pk_{Hqn} , pk_{Hn}), point of inertia analysis, transformations (fourier, wavelet) and so on. These analyses are carried out not only for whole maps (\mathbf{N} , \mathbf{Q} , \mathbf{E}), but also for their parts (pos. / neg. pulses $\mathbf{X}^+ / \mathbf{X}^-$ or pos. / neg. half-waves of voltage $\mathbf{X}_\cap / \mathbf{X}_\cup$). The result is a set of characteristic features called *fingerprint*, which aims to identify a PD source [34].

3. Specimens, test-setup and measurement techniques

Most of the PD measurements were carried out with the test vessel described in [7], using commercial 10/20 kV, 40 A fuses. For easy exchange

of the filler, some of the fuses were fitted with a screwable cab, equipped with sealing joints. One fuse was perforated at the ends to allow application of different gases.

Filler

As base filler commercially available sand (H31 from Quartzwerke, Germany) was used. The filler modifications comprised the addition of

- 10 %, 20 % and 30 % of quartz powder as pore filler,
- 200 ml of $[\text{SiO}_2]_x$ as solidifying pore filler,
- up to 10 % of SiC for stress relieving,
- 10 % of TiO_2 to enhance the dielectric properties of the sand,
- up to 1.3 ml of water (H_2O) for stress relieving.

The modified filler was prepared in a rotating drum. Rotation was stopped, when the mixture was visible homogeneous. In case of quartz powder a special technique was used to suppress segregation of the bi-dispersive grain size fractions.

The filler was applied to the fuses on a vibrating device, until the fuses were completely filled and no more visible settling was achieved.

In case of $[\text{SiO}_2]_x$ and H_2O , the ingredients were supplied to the filler after mounting the fuses and application of the base filler. The specimens were tempered at 150° C for 48 hrs.

Test setup for PD measurements

In addition to the test setup used in [7], a potential free current transformer was inserted, allowing a current to be driven through the fuse, while simultaneous measuring the PD.

The fuses were introduced to the test vessel and the test voltage was applied for 40 min. Eventually current in different amounts (10, 20, 30 and 40 A) were also applied to the fuses.

With voltage applied to the fuse under test, the PD detector was programmed to record impulses over the whole test duration in periods of 1 min. This allows the observation of the temporal PD behavior. The PD-detector consisted of an *ICM-Device* from *Power Diagnostix*, Aachen, Germany, able to record maps of size 256x256 (i.e. 256 windows of charge as well as phase). The recorded maps were read into a program and statistical as well mathematical operations carried out using a *Sun E10k*, equipped with 56 CPUs, 32 GB RAM and 1 TB of storage.

Specimens for switching tests

For switching tests specimens were used consisting of a prototype fuse with characteristic values of 6/12 kV and 630 kVA. The prototypes were

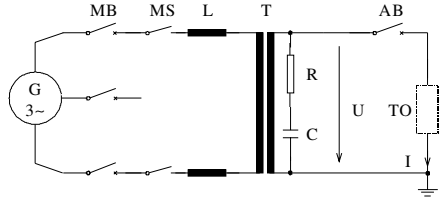


Fig. 4: Test circuit for I_2 -test.

equipped with three band type fusible elements of 600 mm length in parallel, bearing equidistant hole-constrictions in their middle. Filler with quartz powder in different amounts was used.

Setup for switching tests

The setup for the switching tests consisted of a single-phase direct test circuit (Fig. 4). A synchronous generator fed via a master-breaker and a making switch the primary side of a transformer. On its secondary side the fuses were mounted in series with an auxiliary breaker. The latter was used to determine the parameters of the prospective transient recovery voltage (TRV) and the prospective current in preliminary setting tests. During the tests with the fuses (TO) the AB was closed. The inductance L was tuned for a prospective current of $I_2 = 5.6$ kA, R and C were adjusted to form a TRV with a peak value of $u_c = 22$ kV and a rate of rise of 0.11 kV/ μ s as is required by [25]. The making switch served to realize the desired making angle of 10° , while the master-breaker was used to de-energize the test circuit after the test. The power-frequency recovery voltage was adapted to 10.4 kV by the help of the transformer and was applied to the fuses for at least 60 s after arc extinction.

4. Results

PD analysis

Fig. 5 shows a typical distribution of impulses rate vs. apparent charge for an unmodified fuse at the beginning of the test. As can be seen, the positive impulses are slightly preferred. Bipolar logarithmic scaling is used, i.e. two decades of polarity of the PD pulses. The peak at ± 6 nC is caused by the

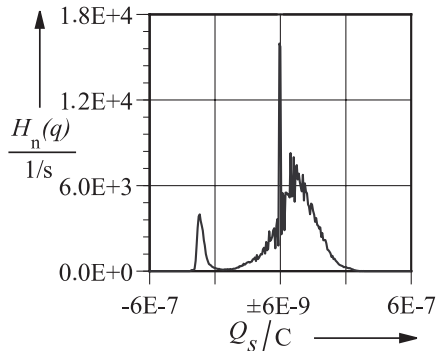


Fig. 5: $H_n(q)$ for unmodified fuses at 20 kV.

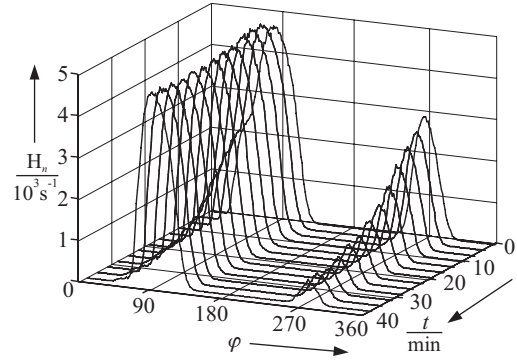
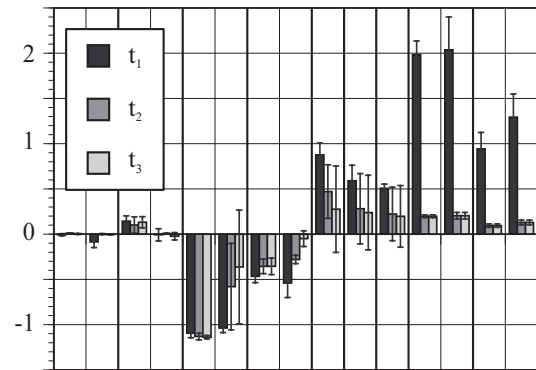


Fig. 6: $H_n(\varphi)$ distribution over time, at 20 kV, 10 A.

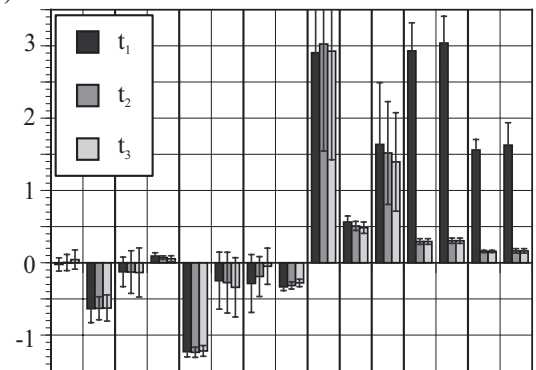
measurement device and discriminated in further data analysis.

If such diagrams are stacked for consecutive measurement intervals, a 3D-view of the PD history results, as shown in Fig. 6 for the impulse rate vs. phase of occurrence $H_n(\varphi)$. Here the strong decay of PD impulses rate over the time becomes obvious, in particular for impulses in the negative half-wave.

Fig. 7 shows PRPD-fingerprints of unmodified fuses at 20 kV, 0 and 40 A, being calculated at 0, 20 and 40 min. of the test duration. The fingerprints resemble to the fault classification “narrow cavity in solid material” and “multiple point-plane



a) sk_{Hqn} sk_{Hn} ku_{Hqn} ku_{Hn} k_{Qkcc} k_{mcc} pk_{Hqn} pk_{Hn}



b) sk_{Hqn} sk_{Hn} ku_{Hqn} ku_{Hn} k_{Qkcc} k_{mcc} pk_{Hqn} pk_{Hn}

Fig. 7: PRPD-fingerprint of fuses at 20 kV and a) 0 A and b) 40 A. $t_1 = 0$, $t_2 = 20$, $t_3 = 40$ min.

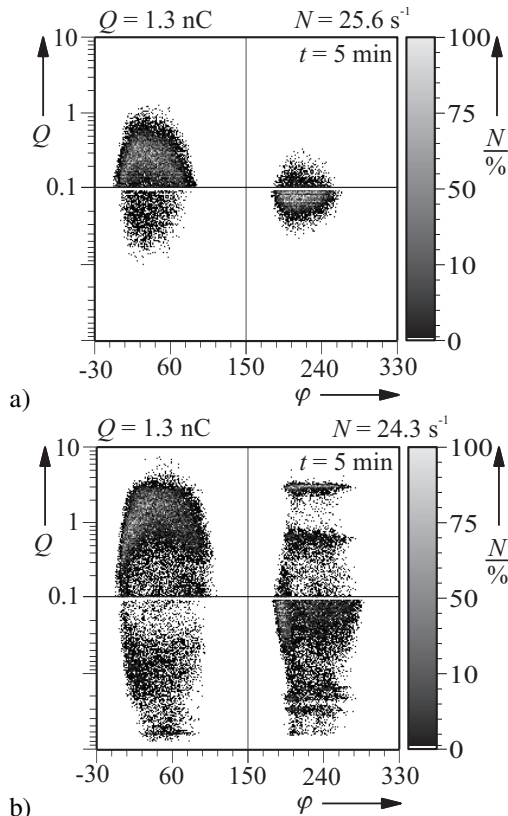


Fig. 8: PD Maps for different gaseous filler components: a) air, b) pure N_2 .

configuration in air” [34], but matching is not absolute. Especially the cross-correlation factor k_Q , which compares the distributions of charge in the positive and negative half-waves, shows strong deviations. As noticeable from the error-bars, the data manifests a strong variation. This is inherent to all the measurements carried out and caused by the complex structure of the filler.

The gaseous component of the filler also affects the PD activity (Fig. 8): In air, a lower level of apparent charge compared to N_2 is found. Also a strong decay of PD activity over the time (e.g. Fig. 6, 9) can be observed. This indicates the formation of ozone (O_3) in samples with air, which reduces electrical field strength due to its dipole character and

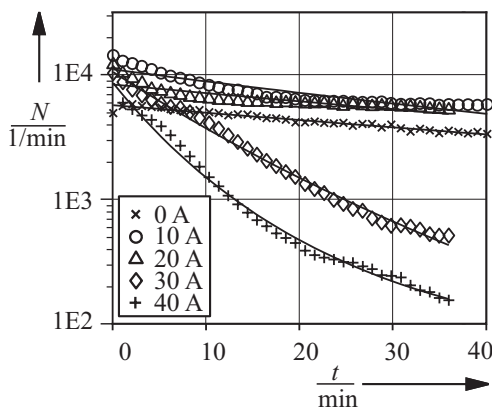


Fig. 9: PD impulse rate at 20 kV and different currents, unmodified filler.

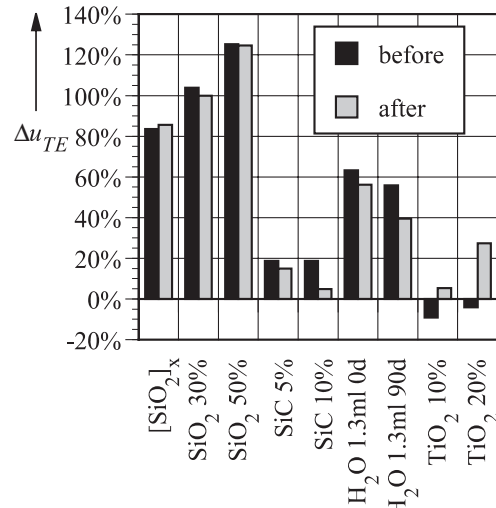


Fig. 10: PD performance of different fillers, before and after 40 min.

therefore decreases PD activity. In case of pure N_2 no O_3 can be formed and no decay in PD activity happens. Comparing the total sum of apparent charge for pos. and neg. half-wave, in N_2 a nearby equal distribution is found, whereas in air a large difference was observed.

The biggest impact on the PD behavior was found, when current was applied to the fuse. Fig. 9 shows the drastic decay in PD activity for different current values. The decay is more pronounced for higher currents, which is explainable by thermal expansion of the filler’s components (i.e. pressure rise in the gas, tighter contact between the grains) and the higher intrinsic conductivity of SiO_2 .

The influence of pore filler on the PD inception voltage u_{TE} becomes obvious in Fig. 10, where the

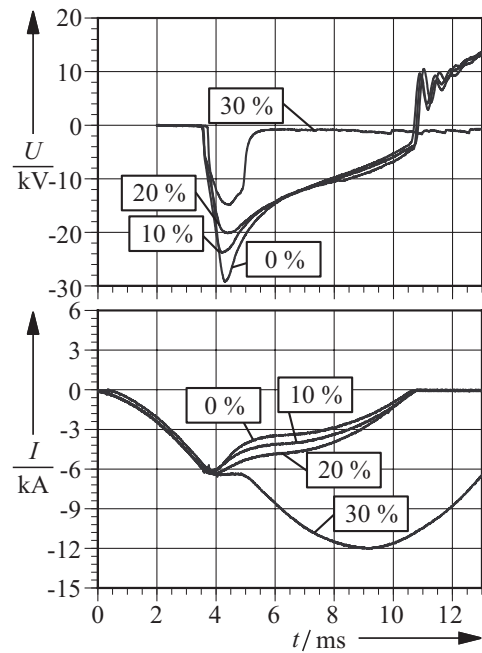


Fig. 11: I_2 -test on fuses with different pore filler amount.

difference in PD inception voltage Δu_{TE} (compared to unmodified filler) is shown. The best performance is achieved with $[\text{SiO}_2]_x$ and quartz powder (SiO_2 in Fig. 10), followed by addition of water (H_2O). The latter shows decreasing performance when measured again after 90 days (H_2O 90d), because water is integrated in the crystal lattice. Worst performance was observed with SiC and TiO_2 .

Switching tests

Fig. 11 summarizes the I_2 -switching behavior of fuses with pore filler. The percentage shows the weight content of the pore filler. Most impressive is the reduction of the switching overvoltage u_{sw} , which decreases from about 30 kV at 0 % pore filler to approx. 14 kV at 30 % pore filler. This is in accordance with [23], where a decrease of the electrical field strength in the arcing channel for smaller sized filler grains was found, but contradicts findings in [10, 16], where a more compact filler leads to higher u_{sw} .

Evaluating the Joule integrals (Fig. 12), no distinguishable differences can be found in the pre-arcing interval. However, the decrease in u_{sw} is attended with higher I^2t -values in the arcing interval: The I^2t -values increase with higher pore filler degree. This is in contrast to [10, 11, 12, 38], where filler with higher compactness or smaller medium particle size is suspected to give lower I^2t -values, but agrees with findings for fuses with small grained filler [9, 13].

Because of the elevated I^2t -values, the fuse has to deal with higher switching energies, therefore production-level fuses have to be carefully designed. At 30 %, the fuses were not able to switch, leading to excessive high values of the arcing Joule-integral.

The misbehavior of the fuse filled with 30 % of pore filler may be explained by the excessive Joule-energy consumed while switching: If Fig. 11 is considered, the current remains nearly constant after ignition of the arc, instead of decreasing as for the fuses with other amounts of filler. After 5 ms, the

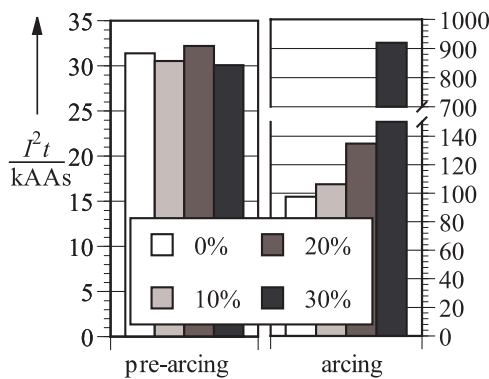


Fig. 12: I^2t -values of fuses with different amount of pore filler in the pre-arcing and arcing interval.



Fig. 13: Fulgurite of a fuse with 30 % of pore filler after I_2 -test.

current increases to the prospective current and the arcing voltage drops to about 500 V, resulting in an overload of the fuse. After the test, only parts of the fuse could be retrieved. The fuses' core showed no clear distinguishable fulgurite. Instead a crumbly, foamy and pumiceous mass was found (Fig. 13), somewhat similar to fulgurites found in fuses with very fine grained filler [23]. This led to the assumption, that the constrictions of the fusible elements – maybe distinct or several windings of the helical filaments too – were short-circuited in the moment of arcing, resulting in an unabridged arc, which could not be cleared.

The short-circuiting of the constrictions and fusible elements windings may be explained by the consistency of the filler. At 30 % pore filler content, the percolation point is reached and the smaller grains of the pore filler embed the larger grains, resulting in a higher mechanical elasticity of the filler, therefore degradation of mechanical stiffness [39]. If arcing occurs, the filler cannot resist the pressure rise in the arc channel [40] and yields away, leading to an unabridged arc.

5. Conclusion

Filler modifications can impede PD generation, but also influence the switching behavior of the fuse. The PD reduction was achieved with different fillers, quartz powder giving the best results.

The PD behavior of fuses was analyzed by use of PRPDA. Fuses manifest a strong decay in PD activity when current is applied. There is also a decay of PD activity over the time, which can be explained by generation of ozone inside the fuse.

The use of bi-dispersive filler not only obstructs PD generation, but also reduces the peak of the

switching overvoltage. This decrease is combined with an increase of arcing energy, which must be considered in the fuse design. A certain level of pore filler addition cannot be exceeded, since the fuses lose their ability to extinct the current.

The concept of bi-dispersive filler has to be investigated further by additional measurements like complete IEC282 type test (I_1 , I_3), long-time tests and determination of the time-current curve, whereas it is known from [41], that time-current characteristic is slightly slower for finer grains.

References

- [1] Sturm M, "Systeme zur zukünftigen Energieoptimierung und -vermarktung I". *Scriptum*, Univ. Hannover, 2003.
- [2] Peier D; Temmen K: "Beurteilung der Degradation von Isolierungen mittels Teilentladungsmessung". *Elektrie* 53(1999), No. 9-10, pp. 314-9, 1999
- [3] Erlenhof A; Grote J; Heiß W; Müller HJ; Siebel KH; Wittek L: "Platzsparender und berührungssicherer Kurzschlußschutz von Transformatoren und Mittelspannungs-Netzstationen". *Elektrizitätswirtschaft*, Vol. 84 (1985), No. 10, pp. 356-70, 1985.
- [4] Dirks R: "Die HH-Sicherung als Herausforderung an den Schaltanlagen-Konstrukteur". *Elektrizitätswirtschaft*, Vol. 87 (1988), No. 16/17, pp. 781-2, 1988
- [5] Walz RD; Büscher A; Primus IF: "Die neue ökonomische 24-kV-Schaltstation, schlüsselfertig am Kranhaken". *Elektrizitätswirtschaft*, Vol. 97 (1998), No. 4, pp. 26-34, 1998.
- [6] Läßle H: "Die neue Hochspannungs-Hochleistungssicherung (HH-Sicherung) der SSW". *Siemenszeitschrift*, Vol. 11, No. 2, pp. 65-70, 1931.
- [7] Gärtner J; Gockenbach E; Borsi H: "Influences of hv-fuses on Partial Discharge Measurement of Electrical Equipment". *ICEFA Turin 1999*, pp. 77-82.
- [8] Paukert J: "Search for new extinguishing media for LV fuses". *ICEFA Eindhoven 1987*, pp. 44-9.
- [9] Turner HW; Turner C: "Phenomena occurring during the extinction of arcs in fuses". *Int. Symp. on switching Arc Phenomena*, Lodz, 1973, pp. 253-6.
- [10] Namitokov KK; Frenkel ZM: "Influence of Quartz-Filler Density on Arc Processes in Fuse". *Electrotechnika* Vol. 54 No. 8, pp. 36-7, 1983.
- [11] Lipski T: "Behaviour of stone-sand fuses in short-circuit conditions". *Proc. 10th Int. Conf. on Gas discharges and their Application*, Swansea, 1992, pp. 204-7.
- [12] Lipski T; Pikon M: "A Comparison of Current Interruption by Sand SiO₂ and Sand SiO₂/Gas SF₆ Fuses". *ICEFA Ilmenau 1995*, pp. 176-9.
- [13] Ossowicki J: "Influence of quartz-filler granulation on breaking D.C. Overloads by Means of Strip Fuses". *Int. Symp. on switching Arc Phenomena*, Lodz, 1973, pp. 262-4.
- [14] Shea JJ; Crooks WR; Smith JDB: "Gas Evolving Materials for Improved Low Current Interruption in High Voltage Current Limiting Fuses". *IEEE Trans. on Power Del.*, Vol. 10, No. 1, pp. 258-65, 1995.
- [15] König D; Trott J; Müller HJ; Müller B: "Switching Performance of High-Voltage Fuse-Elements in Different Solid and Gaseous Filling Media". *ICEFA Eindhoven 1987*, pp. 50-6.
- [16] Ilyina NA; Zhemerov GG; Zaika EI; Shklovsky IG: "The Basic Principles to Engineer a High Quality's Fuses for Power Semiconductor Convertors". *ICEFA Turin 1999*, pp. 315-8
- [17] Saqib MA; Stokes AD: "Characteristics of Fuse Arcing in Different Fillers". *ICEFA Turin 1999*, pp. 275-8.
- [18] Bussière W: "Influence of sand granulometry on electrical characteristics, temperature and electron density during high-voltage fuse arc extinction". *J. Phys. D: Appl. Phys.* 34 (2001), pp. 925-35, 2001.
- [19] Kaltenborn U; Rocks J; Skryten PK: "Löschmedium zum Löschen von Lichtbögen". *Patent application* EP 1 162 640 A1, European Patent Office, Munich, 2001.
- [20] Kroemer H: "Der Lichtbogen an Schmelzleitern in Sand". *Arch. f. Elektrotechnik*, Vol. 36, Iss. 8, Berlin 1942, pp. 455-70.
- [21] Johann H: "Die Lenkung des Schaltvorgangs in Hochspannungs-Sicherungen mit körnigem Löschmittel". *VDE-Fachberichte*, 18(1954), Wuppertal, 1954, pp. 34-8.
- [22] Vermij L: "Electrical behaviour of fuse elements". *PhD*. TH Eindhoven, 1969.
- [23] Huhn P: "Über das Verhalten eines durch Drahtexplosion eingeleiteten Lichtbogens in körnigem Medium". *PhD*. TU Hannover, 1971.
- [24] Eger D: "Ein Beitrag zur mathematischen Modellierung der physikalischen Vorgänge in Hochspannungs-Hochleistungs-Sicherungen". *PhD*. TH Illmenau, 1990
- [25] DIN EN 60282-1: "Hochspannungssicherungen, Teil 1: Strombegrenzende Sicherungen (IEC 60282-1:1984 + A1:1996)". VDE-Verlag GmbH Berlin, 1998.
- [26] Wright A, Newberry PG: "Electric Fuses". Peter Peregrinus Ltd. 1982.
- [27] Chen S: "Research on the Technique of Filling Quartz Sand in Fuse". *ICEFA Eindhoven 1987*, pp. 93-8.
- [28] Ehrhardt A: "Schaltverhalten von Sicherungen bei kleinen Überströmen unter besonderer Berücksichtigung des Wiederspüßens". *PhD*. TU Ilmenau, 1999.
- [29] Wolf I: "Grundlagen und Anwendungen der Maxwellschen Theorie I". *B.I. Hochschultaschenbücher*, Vol. 818, Wissenschaftsverlag, Mannheim, 1968.
- [30] Kreuger FH: "Partial Discharge Detection in High-Voltage Equipment". Butterworths, London, 1989.
- [31] Schichler U: "Erfassung von Teilentladungen an polymerisolierten Kabeln bei der Vor-Ort-Prüfung und im Netzbetrieb". *PhD*. Univ. Hannover 1996
- [32] Suwarno: "A comparison between void and electrical treeing discharges in polyethylene". *Proc. of The 6th Int. Conf on Properties and Applications of Dielectric Materials*, Xi'an, China, pp. 493-6, 2000.
- [33] Okamoto T; Tanaka T: "Novel Partial Discharge Measurement Computer-Aided Measurement System". *IEEE Trans. on El. Ins.*, Vol. E1-21, pp. 1015-9, 1986.
- [34] Galski E: "Computer-Aided Recognition of PD Using Statistical Tools". *PhD*. TU Delft, 1991
- [35] Bartnikas R: "Partial Discharges". *IEEE Trans. Dielect. and Ins.*, Vol. 9, No. 5, pp. 763-808, 2002.
- [36] van Brunt RJ: "Stochastic properties of partial-discharge phenomena". *IEEE Trans. on El. Ins.* Vol. 26, No. 5, pp. 902-48, 1991.
- [37] Hoof M: "Impulsfolgen-Analyse: Ein neues Verfahren in der Teilentladungsdiagnose". *PhD*. UG Siegen, 1997
- [38] Lee S; Kim IS; Han SO: "The Test Method to Acquire the Optimal Parameter for CL-Fuse". *ICEFA Turin 1999*, pp. 265-70.
- [39] Yin H: "Acoustic Velocity and Attenuation of Rocks: Isotropy, Intrinsic Anisotropy, and Stress Induced Anisotropy". *PhD*. Stanford Univ. 1992.
- [40] Jakubluk K; Lipski T: "Dynamics of fulgurite formation during arcing in hrc fuses". *J. Phys. D: Appl. Phys.* 26(1993), pp. 424-430, 1993.
- [41] Trott J: "Untersuchungen zur Lichtbogenlöschung in Hochspannungs-Hybridsicherungen". *PhD*. Darmstadt 1988

Acknowledgments

The authors like to thank EFEN Elektrotechnische Fabrik GmbH, Eltville, Germany, for the manufacturing of the test fuses, SIEMENS AG, Berlin, Germany for carrying out the switching test, and Dipl.-Ing. R. Jochem who did most of the PD measurements.